■Invited Lecture■

High-Fidelity Numerical Simulations of Reacting Flows: Fundamentals and Applications

YOO, Chun Sang

Ulsan National Institute of Science and Technology (UNIST), UNIST-gil 50, Ulsan 689-798, Republic of Korea

Abstract : For high-fidelity numerical simulations of reacting flows supposed to solve compressible Navier-Stokes equations, both acoustics and flows at open boundaries should be carefully taken care of. For this purpose, so-called '3D-NSCBC' and its derivatives have been developed and made progress in clean exit of flows and flames at the boundaries. Due to the development of novel numerical schemes and petascale high-performance computing clusters, direct numerical simulations (DNS) of laboratory-scale turbulent flames can now be simulated. Since the mid 2000's, several 3D DNS of turbulent lifted nonpremixed jet flames in heated coflows have been performed and their stabilization mechanism and flame structures have been figured out. In case of combined experiment and simulation study, high-fidelity simulations of flame-vortex interaction in counterflow and diffusive-thermal instability in oppose tubular nonpremixed flames have also been performed and their characteristics have been investigated by comparing with their experimental counterparts. For more practical applications, ignition characteristics of hydrogen/air, *n*-heptane/air, *iso*-octane/air and primary reference fuel (PRF)/air mixtures under homogeneous charge compression ignition (HCCI) conditions have been elucidated using 2D DNS.

Key words : Direct numerical simulations, Turbulent combustion, Flame instability, Flame-vortex interaction, HCCI

1. Introduction

As global warming and air pollution worsen and the fossil fuel shortage becomes eminent in the near future, the demand for renewable energy and clean and efficient combustion has grown significantly. To meet the demand, several new combustion technologies have been proposed thus far. For instance, homogeneous charge compression ignition (HCCI) engine has emerged as an alternative to conventional diesel and spark-ignition engines due to its high diesel-like fuel efficiency with low emission [1], and a new technology utilizing hydrogen jets issuing into a hot environment has also been proposed to meet the more stringent regulations of NO_x emission in gas turbines [2]. Compared to current engines, combustion processes in these new technologies can be characterized by much higher pressure, lower temperature, and higher levels of dilution air. However, combustion processes in these environments have not been fully understood due to the limitations of experiments and simulations.

Since the beginning of the new millennium, however, direct numerical simulations (DNS) of laboratory-scale turbulent jet flames can now be simulated with detailed kinetic mechanisms in three dimensions and provide a first-principles understanding of such turbulent flames and a database for turbulent combustion modeling [3]. This is primarily attributed to the development of high-performance computing (HPC) clusters and novel numerical methods.

In this paper, so-called 'three-dimensional Navier- Stokes Characteristic Boundary Conditions (3D-NSCBC)' for simulating compressible reacting flows are, first, introduced and then, state-of-the-art 3D DNS of turbulent lifted nonpremixed jet flames in heated coflows are presented and the stabilization mechanisms of such flames are elucidated. As examples of combined experimental and numerical studies, the characteristics of flame-vortex interaction in counterflow and diffusive-thermal instability of opposed tubular nonpremixed flames are also presented. Finally, ignition characteristics of several fuel/air mixtures under homogeneous charge compression-ignition (HCCI) conditions are discussed.

2. 3D-NSCBC

One of the lingering problems in the simulation of compressible Navier-Stokes equations is how to deal with open boundaries, where a significant flow action is present [4,5]. Since Poinsot and Lele [6] proposed the original NSCBC based on locally one-dimensional inviscid (LODI) assumption, numerous simulations of turbulent combustion have been successively performed if the flow does not significantly interact

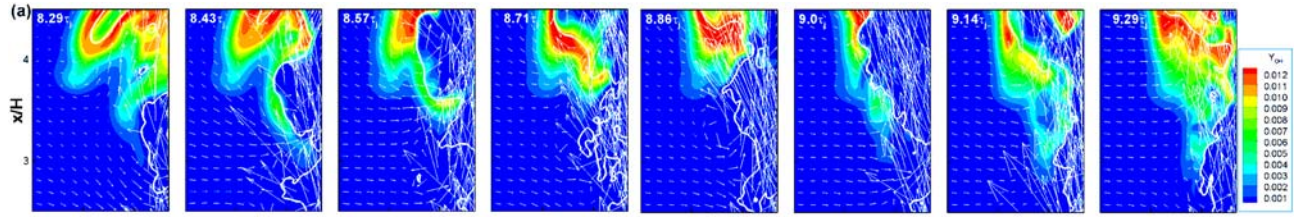

Fig.1 Temporal evolution of isocontours of OH mass fraction of the left branch of turbulent lifted hydrogen jet flame in heated coflow [15].

with the open boundaries, or the boundary is far from the location where turbulent combustion takes place.

However, significant flow distortion may occur when flames, strong vortices, or turbulent eddies pass through the open boundaries [4,5,7]. This is primarily attributed to the fact that at such situations, the flow is no more locally one-dimensional inviscid and as such, multi-dimensional, viscous, and reaction effects may change the flow at the boundaries. To resolve this issue, the transverse, viscous, and chemical reaction source terms are included in the incoming wave amplitude of the characteristic variables. For example, the incoming wave amplitude in the *x*-direction, $L_1^{(x)}$, is defined by [4,5]:

$$L_1^{(x)} = \alpha(p - p_\infty) + aT_{1,\text{exact}}^{(x)} + (1-a)T_1^{(x)} + V_1^{(x)} + S_1^{(x)}, \quad (1)$$

where p is pressure and p_∞ is the target pressure, $T_1^{(x)}$, $V_1^{(x)}$, and $S_1^{(x)}$ are the transverse, viscous, and source terms, respectively. $T_{1,\text{exact}}^{(x)}$ is the target transverse term. α and a are the relaxation factors for pressure and transverse terms, respectively.

From the low Mach number asymptotic analysis, a is found to be the Mach number of the flow [5]. Consequently, Eq. (1) leads to the effective boundary condition:

$$\frac{\partial p}{\partial t} - \rho c \frac{\partial u}{\partial t} = -\frac{\sigma c}{l_x}(p - p_\infty) + \rho c u_\infty \frac{\partial u}{\partial x}, \quad (2)$$

where σ is the damping coefficient and l_x is the domain length in the *x*-direction. In summary, the inclusion of the extra terms in the incoming wave (see Eq. (1)) renders the flow more one-dimensional inviscid at the boundaries by effectively removing the multi-dimensional, viscous, and reaction effects of the flow (see Eq. (2)), which is now called '3D-NSCBC' together with the treatment of corners and edges [8].

The 3D-NSCBC have been extended by deriving the optimal damping coefficient for high speed flows [9] and formulations for clean exit of non-normal flows [10-12].

3. Turbulent Lifted Flames in Heated Coflows

Turbulent lifted jet flames in heated coflow have been widely investigated not only because of their practical importance in commercial applications such as diesel engines and gas turbine combustors, but because of fundamental importance for understanding auto-ignition and partial premixing in turbulent combustion modeling [13-15].

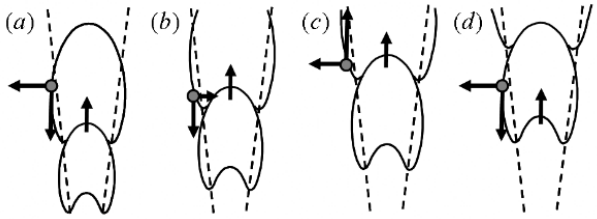

Fig.2 Schematic of the flamebase movement: (*a*) ignition occurs in lean mixtures with low scalar dissipation rate, (*b*) the stabilization point propagates upstream following large flow structure, (*c*) the stabilization point is advected downstream by high axial velocity, and (*d*) ignition occurs in another large flow structure. Gray dot represents the stabilization point and dashed line denotes auto-ignition limit due to low temperature (from Ref. [15]).

After state-of-the-art 3D DNS of turbulent lifted hydrogen jet flame in heated coflow was performed [15], the trilogy of 3D DNS of turbulent lifted jet flames in heated coflows have been performed and their stabilization mechanisms have been elucidated [15-17]. The DNS were performed on Cray XT3 – 5 (Jaguar) in Oak Ridge National Laboratories using the Sandia DNS code, S3D [18].

First, the stabilization mechanism of turbulent lifted hydrogen jet flame in a heated coflow [15] is discussed. The coflow temperature is 1,100 K which is approximately 200 K larger than the crossover temperature of hydrogen/air chemistry. As such, the flame stabilization is primarily achieved by auto-ignition of fuel-lean mixtures where scalar dissipation rate is low and temperature is high enough for auto-ignition. Figure 1 shows the typical movement of the flamebase, exhibiting a cyclic motion due to the balance between consecutive auto-ignitions and large axial velocity of large coherent jet structures. From the study, a four-step flame stabilization mechanism was proposed as shown in Fig. 2.

Second, the stabilization mechanism of turbulent lifted ethylene jet flame in a highly heated coflow is slightly different from that in the hydrogen case, of which typical flame structure is shown in Fig. 3.

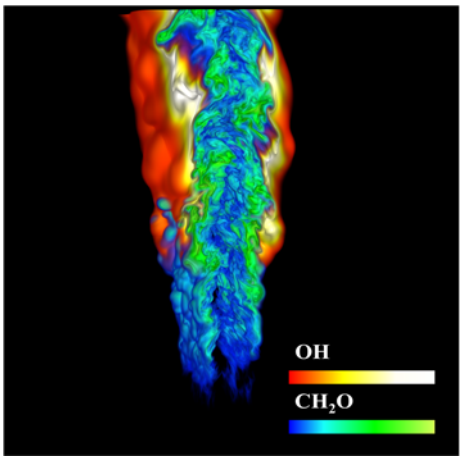

Fig.3 3D volume rendering of OH and CH_2O mass fractions of turbulent lifted ethylene jet flame in a highly heated coflow [16].

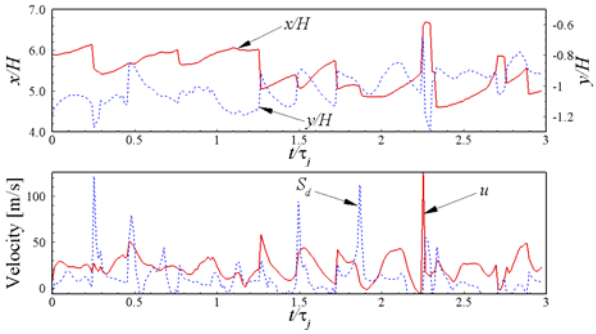

Fig.4 Temporal evolution of the flamebase (top) and the flame normal jet velocity and flame speed (bottom) of turbulent lifted ethylene jet flame in a highly heated coflow [16].

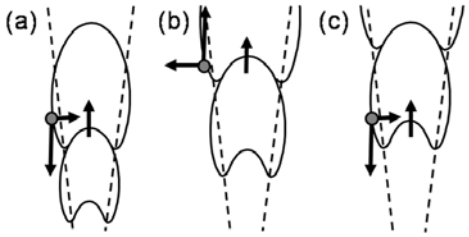

Fig.5 Schematic of the flamebase movement: (*a*) ignition occurs in lean mixtures with low scalar dissipation rate, (*b*) local extinction/flame folding occurs by high scalar dissipation rate and axial velocity and the flamebase is advected dowmstream, and (*c*) ignition occurs in another large flow structure. Gray dot represents the stabilization point and dashed line denotes auto-ignition limit due to low temperature (from Ref. [16]).

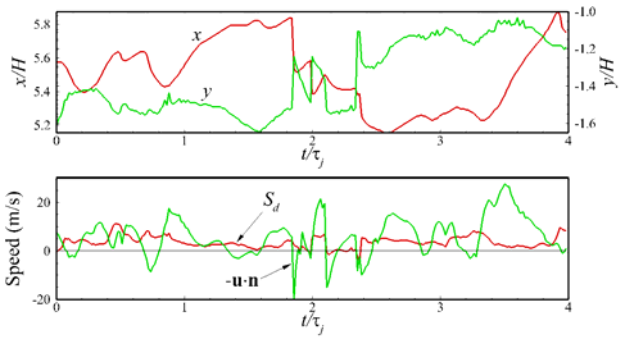

Fig.6 Temporal evolution of the flamebase (top) and the flame normal jet velocity and flame speed (bottom) of turbulent lifted hydrogen jet flame in heated coflow of 750 K [17].

The coflow temperature of 1,550 K is much greater than the auto-ignition temperature and the axial jet velocity is 20 m/s such that auto-ignition at lean mixtures stabilizes the lifted flame but the flamebase is not able to propagate upstream due to the high coflow velocity. These flame and flow characteristics result in a 'saw-tooth' shaped flamebase movement as shown in Fig. 4. Based on the observation of such flamebase movement and consecutive ignition events, a three-step stabilization mechanism was proposed as shown in Fig. 5. Note that there is no flame propagation step in the ethylene jet flame due to the high coflow velocity, which is a big difference between the stabilization mechanisms of the two flames.

As the last of the trilogy of turbulent lifted jet flames in heated coflows, 3D DNS of turbulent lifted hydrogen jet flames in mildly heated coflows were performed with two different coflow temperatures of 750 K and 950 K [17], which are supposed to show the stabilization mechanism without auto-ignition.

In the low coflow temperature case (750 K), the flamebase speed is nearly always positive and exhibits a relatively constant value as shown in Fig. 6. It is, however, readily observed that the flame normal jet velocity varies significantly. These results imply that the short-term flame stabilization is primarily determined by the local jet velocity but the ultimate stabilization location is determined by the balance between the flame propagation speed and local jet velocity of large coherent jet structures. The flame stabilization mechanism and structure of the two flames are now under investigation.

Readers are referred to Ref. [15-17] for detailed analysis of flame stabilization mechanisms and flame structures of the turbulent lifted jet flames in heated coflows. These DNS cases are now being used for development and validation of turbulent combustion models [19-21].

4. Combined experimental and numerical studies

In general, experiments of laminar flames as well as turbulent combustion can still provide limited information such as temperature, chemiluminescence of select species, and overall pollutant emission and hence, detailed characterization of even simple laminar or turbulent flames is still elusive. A combined experimental and numerical study is, therefore, needed to appreciate laminar/turbulent combustion more comprehensively.

Flame-vortex interactions have been widely investigated in the combustion community due to their relevance to turbulence-

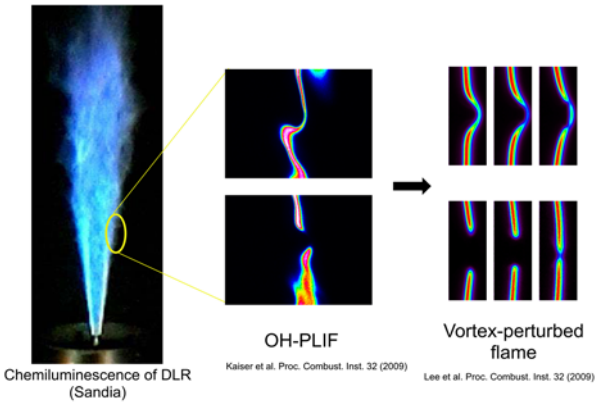

Fig.7 Schematic of modeling flame-turbulence interaction using vortex-perturbed flame in counterflow configuration.

chemistry interaction [22] and are a good example of the combined experimental and numerical studies. In high Reynolds number turbulent jet flames, local extinction can often occur due to locally high scalar dissipation rate or strain rate, resulting in flame holes as shown in Fig. 7 [23]. The flame holes can be recovered by edge flame propagation or re-ignition, depending on local flame/flow conditions [24,25]. These flame-turbulence interactions can systematically be modeled as flame-vortex interaction in counterflow configuration to understand the underlying physicochemical aspects of the interaction (see Fig. 7).

First, the ignition characteristics of diluted hydrogen versus heated air in an axisymmetric counterflow were numerically investigated using S3D [26]. The same experimental study was conducted previously by Seiser et al. [27] and there were still unresolved questions on how much the multi-dimensionality and preferential diffusion would affect the evolution of a nascent ignition kernel. From the simulation, multi-dimensional effect and initial ignition size are found to be the main factors to determine the evolution of the ignition kernel.

Figure 8 shows the temporal evolution of OH LIF signals obtained from the experiment and simulation. The result from 2D axisymmetric simulation of the hydrogen ignition shows a good agreement with the experiment in terms of edge location and overall shape of the flame. Furthermore, it is found from the simulation that the preferential diffusion effect is significant only when the size of the ignition kernel is relatively small due to high curvature effect of the small-size ignition kernel. This is a good example of how the high-fidelity numerical simulations can support experiments and elucidate the underlying physics of a given phenomenon.

Second, the effects of NO and H_2O addition on the dynamics of extinction and re-ignition of vortex-perturbed hydrogen-air diffusion flame were studied both experimentally and numerically [24,25]. In general, it is well known that small

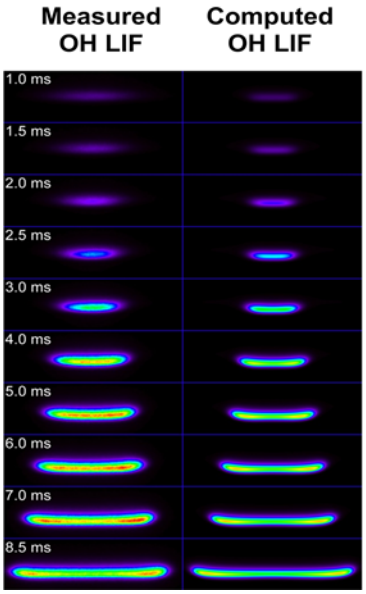

Fig.8 Temporal evolution of OH LIF signals from Ref [26].

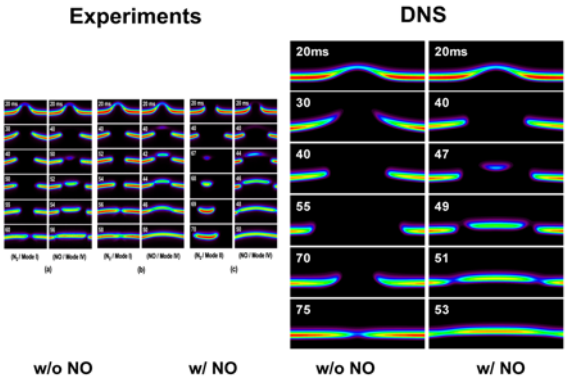

Fig.9 Temporal evolution of OH LIF signals with and without NO addition for comparison of experiments and simulations [25].

amount NO addition into reactants decreases auto-ignition temperature of mixtures due to its catalytic effect on the ignition process and the addition of H_2O lowers the flame temperature, making the flame vulnerable to extinction and difficult to re-ignite.

Figure 9 shows temporal evolution of OH LIF signals from experiments and simulations [25]. The numerical results show a qualitatively good agreement with those of experiments. In addition, the simulations proved that after the extinction by vortex, the recovery of the flame hole depends on the local temperature such that the flame hole is recovered by re-ignition when the local temperature is above the auto-ignition temperature. Otherwise, the flame hole is recovered by the edge flame propagation, which usually takes longer time to finish the recovery process.

It is also found from the simulations that the small amount of H_2O addition does not change the onset of extinction process or

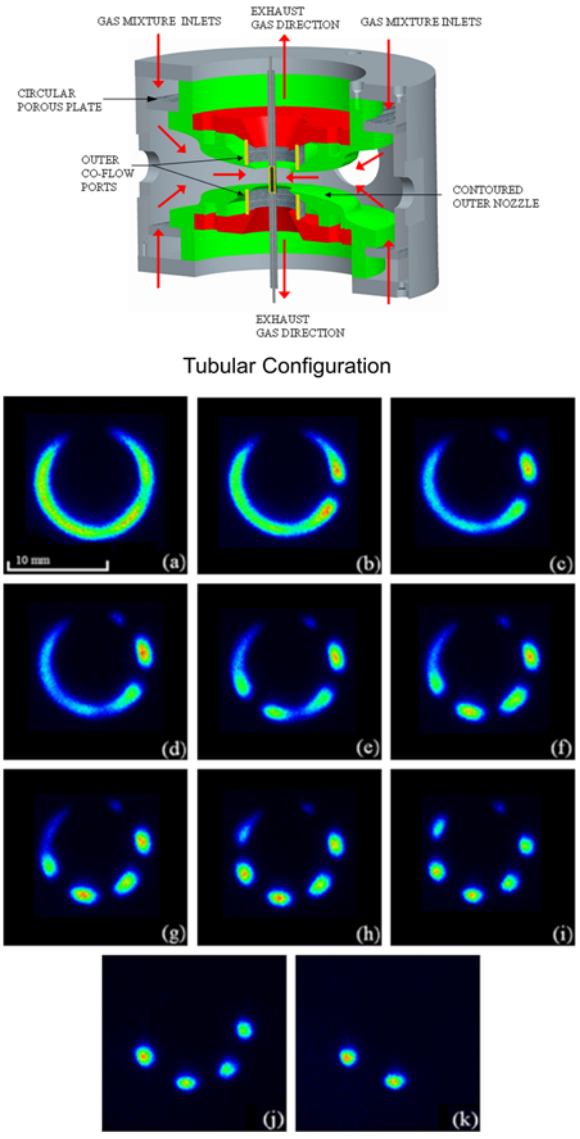

Fig. 10 Schematic of tubular nonpremixed flame burner (top, by courtesy of Prof. R. Pitz) and cell formation with different stretch rates (bottom) from Ref. [30].

the edge flame propagation. However, the H_2O addition delays re-ignition significantly after the extinction by vortex. The chemical inhibition of H_2O is attributed to its relatively large chaperon efficiency in the three-body reaction ($H + O_2 + M \leftrightarrow HO_2 + M$).

As the third example of the combined studies, the diffusive-thermal instability of opposed tubular nonpremixed flames was studied using high fidelity numerical simulations. This study is originated from the works by Pitz and his coworkers [28-30]. Figure 10 shows the schematic of the experimental setup and cellular instability occurring in tubular nonpremixed flames.

By assuming that 1-step overall reaction, constant density, constant radial velocity without azimuthal direction velocity, the governing equations for tubular flame can be modeled as

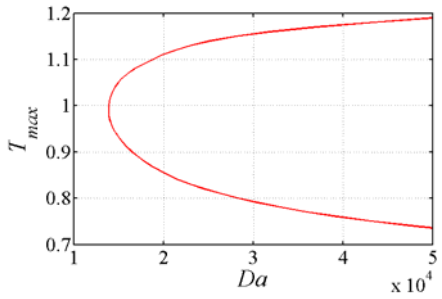

Fig.11 Maximum temperature vs. Damköhler number for 1D tubular flame.

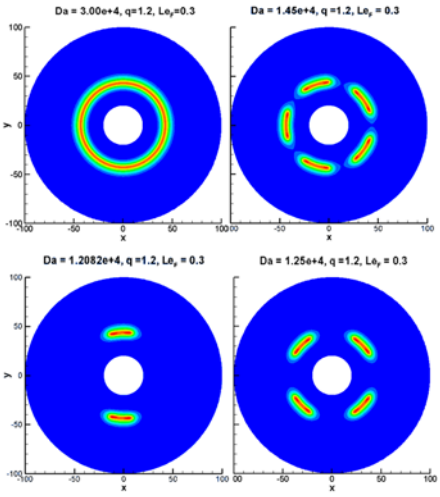

Fig.12 Temperature isocontour of 2D tubular flames with different Damköhler number. Clockwise from top left, Da = 3×10^4, 1.45×10^4, 1.25×10^4, and 1.2082×10^4.

follows:

$$\left(\frac{\partial}{\partial t}+u_r\frac{\partial}{\partial r}\right)\begin{pmatrix}T\\Y_F\\Y_O\end{pmatrix}=\left(\frac{1}{r}\frac{\partial}{\partial r}\left(r\frac{\partial}{\partial r}\right)+\frac{1}{r^2}\frac{\partial^2}{\partial\theta^2}\right)\begin{pmatrix}T\\Y_F/Le_F\\Y_O/Le_O\end{pmatrix}$$
$$+DaY_FY_Oe^{-T_a/T}\begin{pmatrix}q\\-\alpha_FY_{O,2}\\-\alpha_OY_{F,1}\end{pmatrix} \quad (3)$$

where $Le_F(=0.3)$ and $Le_O(=1.0)$ are Lewis number of fuel and oxidizer, respectively, Da is the Damköhler number, q is the heat release rate, and T_a is the activation energy.

First, steady-state 1D tubular flame solutions for a given Damköhler number can be obtained by solving Eq. (3) without the transient and azimuthal terms. Figure 11 shows the maximum temperature of the 1D tubular flame versus Damköhler number, exhibiting a canonical 'C-curve'.

High-fidelity numerical simulations of 2D tubular flames have been performed using the 1D steady tubular flame solutions as the initial conditions. For the simulations, a 4th-order Runge-Kutta method for time integration and the 8th-order central difference scheme for spatial derivatives were

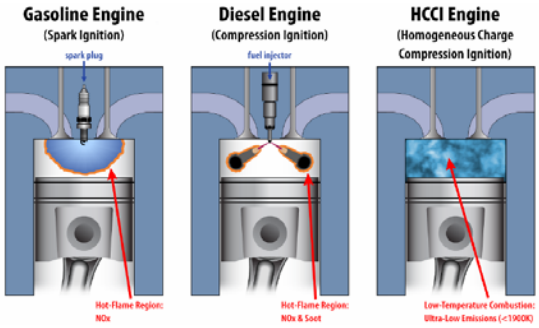

Fig.12 Current and future internal combustion engine concepts from Ref [31].

used with the message passing interface (MPI) for parallel computing.

Figure 12 shows how many the flame cells form with different Damköhler numbers. The flame cells are generated due to diffusive-thermal instability ($Le_F < 1$) of the flames and hence, flame cells are able to survive much lower Damköhler numbers which 1D steady tubular flames cannot survive. The relation between the number of cells, flame location, and Damköhler number is now under investigation.

As a final remark, not only for turbulent combustion but for laminar flames, the high-fidelity numerical simulations are needed to correctly appreciate transient flame-chemistry interactions occurring in flame extinction, ignition, and instability.

5. HCCI Combustion

Homogeneous charge compression-ignition (HCCI) combustion engines have drawn a great attention among engine and combustion researchers since they can provide high diesel-like efficiency with very low nitrogen oxides (NO_x) and particulate emissions [1,31]. As such, HCCI prototype engines are being developed as an alternative to conventional gasoline spark-ignition (SI) and diesel compression-ignition (CI) engines.

Figure 13 shows the concept of HCCI engine characterized by low-temperature combustion and ultra-low emission (< 1900 K) [31]. As indicated in the BES report [31], HCCI combustion occurs primarily through volumetric auto-ignition, largely in the absence of flames under lean, dilute, high-pressure and low-temperature conditions. Therefore, HCCI combustion is primarily controlled by chemical kinetics of the fuel–air mixture.

Up to now, one of the key issues in the development of HCCI engines is how to control the ignition timing and the excessive rate of pressure rise under wide range of load conditions [1]. In particular, an excessive rate of pressure rise under high-load condition can result in engine knock, reducing the engine integrity and hence, must be avoided through careful

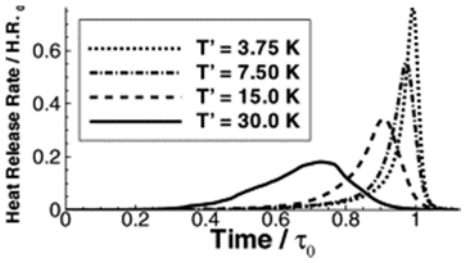

Fig.13 Normalized mean heat release rate versus time of ignitions of hydrogen/air mixture under HCCI condition from Ref [34].

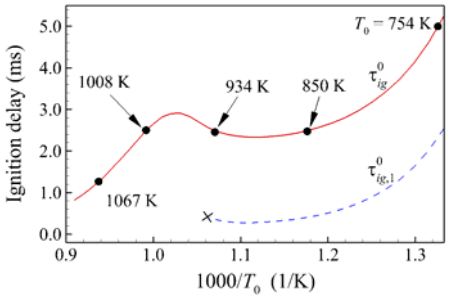

Fig.14 Homogeneous ignition delay of *n*-heptane/air mixture (ϕ = 0.3) at a constant volume with initial pressure of 40 atm as a function of initial temperature [36].

engine design and operation. To smooth out the rate of pressure rise and control the ignition-timing, mixture stratification including temperature and composition inhomogeneities has been proposed [1,31].

The ignition characteristics of hydrogen/air mixtures with temperature inhomogeneities under HCCI conditions have been extensively studied using 2D DNS [32-35]. From the studies, it is confirmed that large temperature fluctuations can effectively reduce the excessive rate of pressure rise by inducing more deflagrative combustion rather than spontaneous auto-ignition in HCCI combustion as shown in Fig. 13. In addition, the overall combustion of hydrogen/air mixture is enhanced with increasing temperature fluctuations.

However, the ignition of hydrocarbon fuel/air mixture under HCCI conditions may exhibit different characteristics due to the existence of negative temperature coefficient (NTC) behavior of hydrocarbon mixtures under high pressure. Figure 14 shows a typical NTC behavior of ignition of *n*-heptane/air mixture. It is readily found that around $T_0 = 934\,\mathrm{K}$, the ignition delay increases with increasing initial temperature.

A DNS study of ignition of a lean *n*-heptane/ air mixture with different mean and root-mean-square (RMS) of temperature under HCCI condition revealed that when the mean temperature lies within the NTC regime, temperature fluctuation retards overall HCCI combustion, while it enhances the overall combustion when the mean temperature is sufficiently greater than the temperature in the NTC regime as shown in Fig. 15 [36].

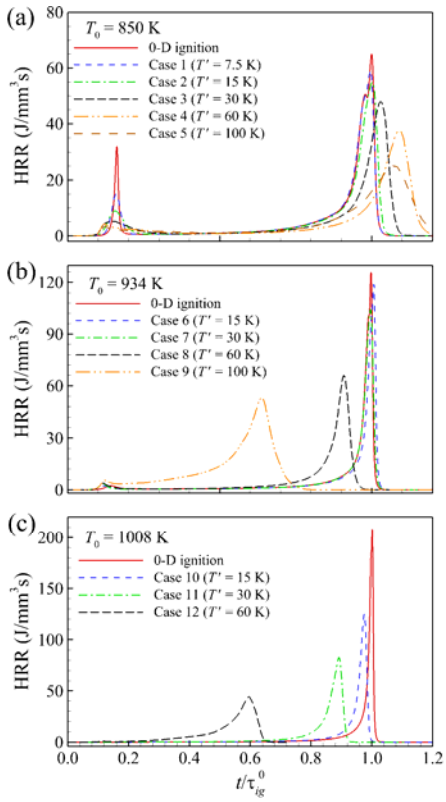

Fig.15 Temporal evolution of mean heat release rate with different RMS for different initial mean temperatures from Ref. [36].

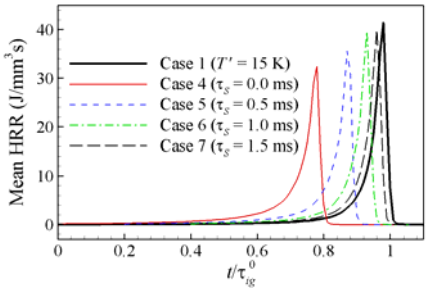

Fig.16 Temporal evolution of mean heat release rate of an *iso*-octane/air mixture at a constant volume with different ignition timings [37].

In addition to temperature inhomogeneities, spark-assisted compression ignition (SACI) combustion has been proposed as one of the remedies to control the ignition timing and the pressure rise rate [37]. In a recent DNS study [37], it is found that SACI combustion can control the ignition timing more precisely than HCCI combustion with temperature inhomogeneities as shown in Fig. 16. Furthermore, compared to HCCI combustion, high turbulent intensity in the SACI condition significantly enhances the overall combustion by inducing many deflagration waves during the early stage of ignition as shown in Fig. 17.

Now, the characteristics of ignition of primary reference fuel (PRF)/air mixtures under HCCI condition are being investigated using 2D DNS.

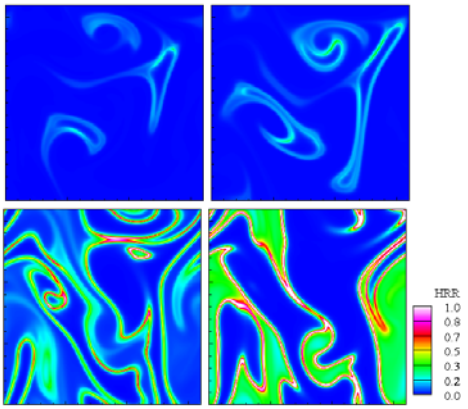

Fig.17 Isocontours of normalized heat release rate with high turbulent intensity at different times [37].

6. Concluding Remarks

The high-fidelity numerical simulations of laminar/turbulent reacting flows have emerged as one of the key research tools for combustion study with the aid of the development of new numerical methods and high performance computing clusters. The novel numerical methods include improved boundary conditions such as 3D-NSCBC and chemistry reduction techniques such as the direct relation graph (DRG) method (not introduced here).

State-of-the-art 3D DNS of turbulent lifted jet flames in heated coflows with realistic chemistry were introduced, which have answered unresolved questions regarding fundamental combustion phenomena. The 3D DNS data is now being used by turbulent combustion modelers to develop and validate their combustion models and these efforts will be more solidified in the future TNF workshop by incorporating DNS and experimental data. In addition, the combined experimental and numerical studies of flame/vortex interaction and cellular instability using high-fidelity numerical simulations were introduced.

2D DNS of ignition of various fuel/air mixtures under HCCI and SACI conditions were introduced and the effects of temperature inhomogeneities, ignition timing, and turbulence on the overall combustion were elucidated. Large temperature inhomogeneities alleviate the excessive rate of pressure rise in HCCI and SACI combustion, and early spark-ignition is able to control the overall ignition timing of SACI combustion.

In the future, DNS of turbulent combustion will incorporate more complex chemistry of large hydrocarbon fuels and more complicated geometry of combustors to simulate more realistic combustion. In addition, the capability of solving multi-physics problems such as spray, two-phase flow, supercritical flow, catalytic reaction, and high Mach number flow will be utilized in DNS.

Acknowledgments

The author was supported by Basic Science Research Program through the National Research Foundation of Korea (NRF) funded by the Ministry of Education, Science and Technology (No. 2012-0003222) and the Human Resources Development of the Korea Institute of Energy Technology Evaluation and Planning (KETEP) grant funded by the Korea government Ministry of Knowledge Economy (No. 2011 -4030200010)

References

1. Dec, J. E., *Proc. Combust. Inst. 32*:2727-2742 (2009).
2. Grout, R. W., Gruber, A., Yoo, C. S., and Chen, J. H., *Proc. Combust. Inst. 33*: 1629-1637 (2011).
3. Chen, J. H., *Proc. Combust. Inst. 33*: 99-123 (2011).
4. Yoo, C. S., Wang, Y., Trouvé, and Im, H. G., *Combust. Theory Model. 9*: 617-646 (2005).
5. Yoo, C. S. and Im, H. G., *Combust. Theory Model. 11*: 259-286 (2007).
6. Poinsont, T. J. and Lele, S. K., *J. Comp. Phys.101*:104-139 (1992).
7. Sutherland, J. C. and Kennedy, C. A., *J. Comp. Phys. 191*: 502-524 (2003).
8. Lodato, G., Domingo, P., and Vervisch, L., *J. Comp. Phys. 227*: 5105-5143 (2008).
9. Liu, Q. L. and Vasilyev, O. V., *Int. J. Num. Methods Fluids 62*:24-55 (2010).
10. Albin, E., D'Angelo, Y., and Vervisch, L., *Comp. Fluids 51*:115-126 (2011).
11. Lodato, G., Ham, F., and Pitsch, H., *AIAA J. 50*: 1291-1306 (2012).
12. Coussement, A., Gicquel, O., Caudal, J., Fiorina, B., and Degrez, G., *J. Comp. Phys. 231*:5571-5611 (2012).
13. Mastorakos, E., *Prog. Energy Combust. Sci. 35*:57-97 (2009).
14. Cabra, R., Myhrvold, T., Chen, J. Y., Dibble, R. W., Karpetis, A. N., and Barlow, R. S., *Proc. Combust. Inst. 29*: 1881-1888 (2002).
15. Yoo, C. S., Sankaran, R., and Chen, J. H., *J. Fluid Mech. 640*:453-481 (2009).
16. Yoo, C. S., Richardson, E. S., Sankaran, R., and Chen, J. H., *Proc. Combust. Inst. 33*:1619-1627 (2011).
17. Yoo, C. S. and Chen, J. H., 3-D DNS of turbulent lifted hydrogen jet flames in mildly-heated coflows, *13th international conference on numerical combustion, Corfu, Greece, Apr. 27 ~ 29*, 2011.
18. Chen, J. H., et al., *Comput. Sci. Disc. 2*:015011 (2009).
19. Richardson, E. S., Yoo, C. S., and Chen, J. H., *Proc. Combust. Inst. 32*:1695-1703.
20. Knudsen, E., Richardson, E. S., Doran, E. M., Pitsch, H., and Chen, J. H., *Phys. Fluids 24*:055103 (2012).
21. Cleary, E. M., Yoo, C. S., and Blanquart, B., *Combust. Flame*, submitted (2012).
22. Renard, P. -H., Thévenin, D., Rolon, J. C., and Candel, C., *Prog. Energy Combust. Sci. 26*:225-282 (2000).
23. Kaiser, S. A. and Frank, J. H., *Proc. Combust. Inst. 32*: 1639-1646 (2009).
24. Lee, U. D., Yoo, C. S., Chen, J. H., and Frank, J. H., *Proc. Combust. Inst. 32*:1059-1066 (2009).
25. Lee, U. D., Yoo, C. S., Chen, J. H., and Frank, J. H., *Combust. Flame 157*:217-229 (2010).
26. Yoo, C. S., Chen, J. H., and Frank, J. H., *Combust. Flame 156*:140-151 (2009).
27. Seiser, R., Frank, J. H., Liu, S., Chen, J. H., Sigurdsson, R. J., and Seshadri, K., *Proc. Combust. Inst. 30*:423–430 (2005).
28. Hu, S., Pitz, R. W., and Wang, Y., *Combust. Flame 156*: 90-98 (2009).
29. Shopoff, S. W., Wang, P., and Pitz, R. W., *Combust. Flame 158*:876-884 (2011).
30. Shopoff, S. W., Wang, P., and Pitz, R. W., *Combust. Flame158*:2165-2177 (2011).
31. Basic Research Needs for Clean and Efficient Combustion of 21st Century Transportation Fuels (2006), available from http://science.energy.gov/~/media/bes/pdf/reports/files/ctf_rpt.pdf
32. Sankaran, R., Im, H. G., Hawkes, E. R., and Chen, J. H., *Proc. Combust. Inst. 30*:875-882 (2005).
33. Chen, J. H., Hawkes, E. R., Sankaran, R., Mason, S. D., and Im, H. G., *Combust. Flame 145*:128-144 (2006).
34. Hawkes, E. R., Sankaran, R., Pébay, and Chen, J. H., *Combust. Flame 145*:145-159 (2006).
35. Bansal, G. and Im, H. G., *Combust. Flame 158*:2015-2112 (2011).
36. Yoo, C. S., Lu, T., Chen, J. H., and Law, C. K., *Combust. Flame 158*:1727-1741 (2011).
37. Yoo, C. S., Luo, Z., Lu, T., Kim, H., and Chen, J. H., *Proc. Combust. Inst* (2012), http://dx.doi.org/10.1016.j.proci.2012.05.019.